Collective excitations in molten iron above the melting point: A generalized collective-mode analysis of simulations with embedded-atom potentials

Taras Bryk[1,2] and A. B. Belonoshko[3]

[1]*Institute for Condensed Matter Physics of the National Academy of Sciences of Ukraine, 1 Svientsitskii Street, UA-79011 Lviv, Ukraine*

[2]*Institute of Applied Mathematics and Fundamental Sciences, National Technical University of Lviv, UA-79013 Lviv, Ukraine*

[3]*Condensed Matter Theory, Department of Theoretical Physics, KTH Royal Institute of Technology, SE-10691 Stockholm, Sweden*

(Received 5 June 2012; published 19 July 2012)

It is shown, that the embedded-atom potential nicely describing structural properties of high pressure Fe [A. B. Belonoshko *et al.*, Phys. Rev. Lett. **84**, 3638 (2000)] can be successfully used for description of collective dynamics of liquid iron. A combination of molecular dynamics simulations and a fit-free analysis based on the approach of generalized collective modes (GCM) is used for calculations of spectra of collective excitations and relaxing modes at 1843 K. The obtained spectrum of acoustic excitations in the long-wavelength region perfectly agrees with the experimental speed of sound and reproduces the dispersion estimated from inelastic X-ray scattering (IXS) experiments [S. Hosokawa *et al.*, Phys. Rev. B **77**, 174203 (2008)]. Heat fluctuations in liquid Fe were studied and resulted in calculated ratio of specific heats $\gamma \approx 1.40$ being in agreement with the IXS-experiment estimate. We report analysis of the wave-number dependence of relaxation processes and their contributions to dynamic structure factors. This permits estimation of most important relaxation processes contributing to the shape of dynamic structure factors of liquid Fe in different regions of wave numbers.

DOI: 10.1103/PhysRevB.86.024202 PACS number(s): 61.20.Ja, 61.20.Lc, 62.60.+v

I. INTRODUCTION

The properties of iron in liquid and solid states are of great importance for geophysical science due to their abundant presence in the outer and inner Earth cores. Structural, electronic, and transport properties of iron were intensively studied in wide ranges of temperatures and pressures experimentally[1–8] and by computer simulations.[9–21]

The choice of effective potentials for classical MD simulations is crucial for correct reproduction of structural and transport properties of transition metals. One of the most successful type of effective potentials for iron is the embedded-atom potentials with parameters estimated from a fit to *ab initio* linear muffin-tin orbital (LMTO) results of energy-volume dependence for hcp and liquid iron.[12] Application of this effective potential to high-pressure liquid iron demonstrated nice reproduction of the experimentally determined structure factor calculations up to the highest pressure of 58 GPa.[14]

Previous simulation studies of dynamic properties of liquid iron at high pressures were focused mainly on calculations of transport coefficients[11,14,15,22] and estimation of speed of sound along the *ab initio* derived Hugoniot pressure-volume curve.[23] The phonon dispersion curves[16,24] and vibrational density of states[13,18] were reported only for solid iron. Collective excitations in liquid Fe so far were not studied by MD simulations, although there were reported simulations of dynamic properties with embedded-atom potentials for molten Ni[25,26] and compared later on with IXS experiments.[27] Recently, there appeared two reports on inelastic x-ray scattering experiments performed on liquid Fe at the temperature of 1570 °C.[7,8] The dispersion $\omega(k)$ of collective excitations, obtained in these scattering experiments had a linear long-wavelength region with the slope that was close to the adiabatic speed of sound 3800 m/s.[2] Another important result of the IXS experiments was the fact that analysis of the Landau-Placzek ratio led to the estimated value of the ratio of specific heats $\gamma = C_p/C_v$ close to 1.4. The ratio of specific heats is a very important quantity for dynamics of liquids because it is a measure of coupling between thermal and viscous processes and, namely, γ is responsible for the relative intensity of the central peak of dynamic structure factor $S(k,\omega)$.[28–30]

It is not a simple task to calculate the dispersion of collective excitations in liquids. In contrast to crystals or glasses, where the atoms are supposed to vibrate around the equilibrium positions, in liquids, there are no stable local equilibrium positions for atoms because they take active part in different relaxation processes: structural relaxation, diffusion, and heat transfer. The methodology of theoretical study of collective excitations in liquids must be based on generalized hydrodynamics. This permits to study viscous regime on macroscopic distances and elastic properties like in solids on meso- and microscopic spatial scales. There exist a few schemes of generalization of hydrodynamics,[28] however, for the purpose of calculations of dispersion of collective excitations from MD data, mainly, a fit based on the memory function formalism[31–35] was applied. Another approach within the mode coupling theory was suggested recently,[36,37] having as an input only information on static structure factors $S(k)$. However, heat fluctuations in this scheme are completely ignored that corresponds to viscoelastic description of liquids with γ close to unity.

One of the most advanced methods of generalized hydrodynamics that was namely developed for the purpose of theoretical analysis of time correlation functions obtained in MD simulations is the approach of generalized collective modes (GCM).[38,39] This theoretical approach is based on systematic extension of the set of hydrodynamic (conserved) variables by orthogonal to them ones, that are supposed to describe correctly more short-time collective processes in comparison with most slow hydrodynamic ones. The extended set of N dynamic variables is then used for calculation of a $N \times N$ generalized

hydrodynamic matrix $\mathbf{T}(k)$, eigenvalues of which correspond to either relaxing (real eigenvalues) or propagating (pairs of complex-conjugated eigenvalues) modes that can exist in the system. Since the hydrodynamic set of dynamic variables contains energy (or heat) density, the GCM approach is able to reproduce correctly all the features of crossover between leading thermal relaxation in the long-wavelength region and structural relaxation on the boundary of hydrodynamic regime as well as the connected with this crossover so-called "positive dispersion" of acoustic excitations.[40]

Hence the aim of this study was to perform MD simulations of liquid iron at the conditions of the IXS experiments[7] and calculate spectra of collective excitations in liquid Fe avoiding any fit. Comparison of the obtained quantities with experimental estimates can show whether the embedded-atom model (EAM) effective potential is able to describe correctly the collective dynamics in liquid iron at low pressures.

II. MOLECULAR DYNAMICS SIMULATIONS AND METHODOLOGY OF ANALYSIS

Using the EAM potential with parameters suggested in Ref. 12, we performed molecular dynamics simulations having a system of 1000 particles in a cubic box under periodic boundary conditions. First, we applied the NPT ensemble to get the equilibrium volume for the system at ambient pressure and temperature $T = 1843$ K that corresponded to the temperature of IXS experiment.[7] During the second stage, the obtained system in a cubic box with the boxlength $L = 23.569$ Å was equilibrated over 40 ps in constant volume and temperature NVT ensemble. The Nose-Hoover thermostat with relaxation time of 0.5 ps was used for the temperature control. The time step in simulations was 2 fs, and the production run was of 100 000 time steps. Sixty wave numbers in the range 0.267–4.461 Å^{-1} were sampled, and the average of static and time-dependent quantities over all possible directions of wave vectors with the same module was performed.

For the need of calculations of time correlation functions and their GCM analysis, we sampled from MD data the following Fourier components of microscopic hydrodynamic variables: the density of particles

$$n(k,t) = \frac{1}{\sqrt{N}} \sum_{i=1}^{N} e^{-i\mathbf{k}\mathbf{r}_i}, \tag{1}$$

the density of mass current

$$\mathbf{J}(k,t) = \frac{m}{\sqrt{N}} \sum_{i=1}^{N} \mathbf{v}_i e^{-i\mathbf{k}\mathbf{r}_i}, \tag{2}$$

that was easily projected onto longitudinal $J^L(k,t)$ and transverse $J^T(k,t)$ components, and energy density

$$e(k,t) = \frac{1}{\sqrt{N}} \sum_{i=1}^{N} \varepsilon_i e^{-i\mathbf{k}\mathbf{r}_i}, \tag{3}$$

where the single-particle energies were calculated in the following way:

$$\varepsilon_i = \frac{1}{2} m v_i^2 + \frac{1}{2} \sum_{j \neq i}^{N} \Phi(r_{ij}) + F(\rho_i). \tag{4}$$

Here, $\Phi(r)$ is the pairwise interaction between atoms i and j at interatomic distance r. $F(\rho)$ is the embedding function that depends on local electron density ρ. The dynamic variable of heat density (that is orthogonal to instantaneous particle density) can easily be obtained as follows:

$$h(k,t) = e(k,t) - \frac{\langle e_k n_{-k} \rangle}{\langle n_k n_{-k} \rangle} n(k,t). \tag{5}$$

The brackets in Eq. (5) mean the ensemble average.

The analysis of time correlation functions calculated in MD simulations was performed by the GCM approach using a five-variable extended set of dynamic variables:

$$\mathbf{A}^{(5)}(k,t) = \{n(k,t), J^L(k,t), h(k,t), \dot{J}^L(k,t), \dot{h}(k,t)\}, \tag{6}$$

where the dotted variables mean the first time derivative of corresponding hydrodynamic variable. For the case of transverse dynamics, the two-variable extended model

$$\mathbf{A}^{(2T)}(k,t) = \{J^T(k,t), \dot{J}^T(k,t)\} \tag{7}$$

was used. Since in classical mechanics the instantaneous cross correlations between a dynamic variable and its first time derivative is equivalent zero, the five-variable dynamic model corresponds to the extension of hydrodynamics by two orthogonal dynamic variables. Namely, these extended variables describe microscopic processes that cannot be obtained by hydrodynamic approach. We would like to mention that the hydrodynamics is essentially the continuum approach and microscopic extension like dynamic model (6) permits to describe correctly effect beyond the continuum picture, i.e., when atomistic structure and dynamics play important role. The analytical solutions of the dynamic models (6) and (7) in the long-wavelength limit were obtained in Refs. 41 and 42, respectively. They will be used for analysis of obtained GCM eigenvalues in the long-wavelength region.

The generalized hydrodynamic matrix $\mathbf{T}(k)$[38] was calculated for both dynamic models (6) and (7) for each k point sampled in MD. Corresponding eigenvalues were estimated and from the imaginary parts of complex eigenvalues the dispersions of collective excitations were obtained. The eigenvectors associated with relevant eigenvalues were analyzed with the purpose to estimate the mode contributions to the time correlation functions (or dynamic structure factors) of interest.

III. RESULTS AND DISCUSSION

A. Structural properties and generalized thermodynamic quantities

The structure factor of liquid Fe calculated as the density-density statistical average

$$S(k) \equiv F_{nn}(k, t = 0) = \langle n_k n_{-k} \rangle$$

is shown in the top panel of Fig. 1. The obtained smooth dependence $S(k)$ gives evidence of good statistics in calculations of static averages. The first sharp diffraction peak of $S(k)$ is located at k 3.05 Å and has the amplitude close to 2.4 that is in reasonable agreement with experimental $S(k)$.[6]

Since in MD simulations we estimated the energy fluctuations in liquid Fe, we were able to study wave-number-

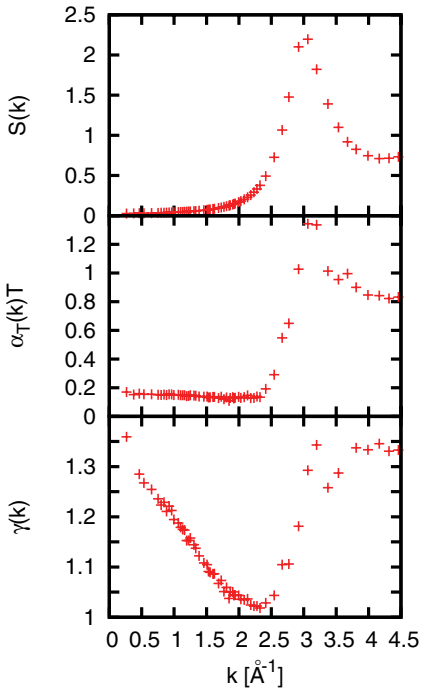

FIG. 1. (Color online) Generalized thermodynamic quantities for liquid iron at 1843 K: structure factor (isothermal compressibility) $S(k)$, linear thermal expansion coefficient $\alpha_T(k)$, and ratio of specific heats $\gamma(k)$. The generalized wave-number dependent quantities tend in the $k \to 0$ limit to their regular macroscopic values.

dependent generalized thermodynamic quantities like linear thermal expansion coefficient $\alpha_T(k)$, specific heats $C_p(k)$ and $C_v(k)$, and their ratio $\gamma(k)$.[38,43] In the long-wavelength limit, these generalized thermodynamic quantities tend to their macroscopic values. In the middle and bottom panels of Fig. 1, the wave number dependencies of dimensionless quantity $\alpha_T(k)T$ and the ratio of specific heats $\gamma(k)$ are shown. Both wave number dependencies show pronounced peaks at the location of the first sharp diffraction peak of $S(k)$, similarly as it was observed for other liquid metals. In the long-wavelength limit, the $\alpha_T(k)$ tends to a value $\sim 9.0 \times 10^{-5}$ K^{-1}, that is, in agreement with the experimental value.[2] The wave-number dependence of $\gamma(k)$ tends to a macroscopic value of the ratio of specific heats ~ 1.4, that is right the value reported in Ref. 7 from analysis of the Landau-Placzek ratio in IXS experiments. It should be mentioned that in Ref. 7, the expected value of γ calculated by using the known experimental values of heat capacity, temperature, volume, thermal expansion coefficient, and adiabatic compressibility was 1.72, which was very close to the value of $\gamma = 1.8$ for liquid Fe at the melting point.[44] Indeed, for liquid metals, the values of specific heats and transport coefficients estimated from the scattering experiments and MD simulations usually are essentially smaller than the values obtained from calorimetric experiments or measurements of kinetic properties. The scattering experiments and MD simulations reflect only the atomic contribution to the dynamic properties that explains the smaller values of γ obtained from the Landau-Placzek ratio. Our estimated value of γ being in good agreement with the IXS experiments[7] is the evidence that the embedded atom potential used in the present simulations of liquid Fe correctly reproduces energy and heat fluctuations.

B. Time correlation functions

Time-correlation functions, calculated in MD simulations, keep all the information on dynamic processes that occur in the liquid on different spatial and time scales. Sampling of energy fluctuations for liquid Fe made possible calculations not only standard density-density time correlation functions, but density-energy and energy-energy time correlation functions too. Namely, these three time correlation functions are called as hydrodynamic time correlation functions, and associated with them correlation times contain the information on the transport coefficients.[45]

In order to understand what kind of processes contribute to the shape of these time correlation functions, one has to perform theoretical analysis based on some model of generalized hydrodynamics. As we stated above, the GCM approach avoids any free fit to the MD-derived time correlation functions. For analysis of hydrodynamic time-correlation functions that reflect longitudinal dynamics, we use the five-variable dynamic model (6) known as thermoviscoelastic one.[40] Using eigenvectors associated with the eigenvalues $z_\alpha(k)$ of the 5×5 generalized hydrodynamic matrix $\mathbf{T}(k)$, the theoretical replicas of hydrodynamic time correlation functions is represented as follows:

$$F_{ij}^{(5)}(k,t) = \sum_{\alpha=1}^{5} G_{ij}^{\alpha}(k) e^{-z_\alpha(k)t}, \qquad i,j = n,e, \tag{8}$$

where each term corresponds to a contribution from a collective mode $z_\alpha(k)$, and the mode amplitudes $G_{ij}^{\alpha}(k)$ are in general case complex numbers. The analysis of mode contributions is more convenient to perform with real amplitudes, therefore, in Ref. 46 it was shown, how in general, the form (8) is reduced to the hydrodynamic-like expression[45] with real amplitudes of mode contributions,

$$\frac{F_{ij}^{(5)}(k,t)}{F_{ij}(k,t=0)} = \sum_{\alpha=1}^{3(1)} A_{ij}^{\alpha}(k) e^{-d_\alpha(k)t} + \sum_{\alpha=1}^{1(2)} \left[B_{ij}^{\alpha}(k) \cos(\omega_\alpha(k)t) + D_{ij}^{\alpha}(k) \sin(\omega_\alpha(k)t) \right] e^{-\sigma_\alpha(k)t}, \tag{9}$$

with real k-dependent amplitudes of mode contributions: from relaxation processes $A_{ij}^{\alpha}(k)$, symmetric $B_{ij}^{\alpha}(k)$ and asymmetric $D_{ij}^{\alpha}(k)$ contributions from αth collective excitation. This expression is the direct extension of the hydrodynamic time correlation functions on the case of existing nonhydrodynamic relaxing and propagating modes. These amplitudes of mode contributions keep all the information about the strength of different collective processes in various windows of wave numbers. Within the GCM approach, the wave-number-dependent amplitudes of mode contributions are estimated in a fit-free way solely from the eigenvector analysis. The different numbers of the exponential and oscillating terms in Eq. (9) reflects the fact that the dynamic model (6) is able to describe solutions with two types of propagating modes.

In Fig. 2, we show the comparison of MD-derived hydrodynamic time correlation functions $F_{nn}(k,t)$, $F_{ne}(k,t)$, and

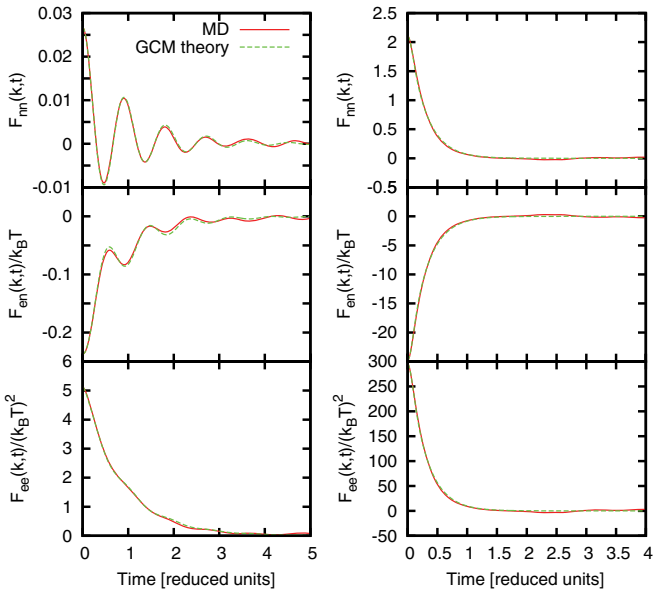

FIG. 2. (Color online) Time-correlation functions obtained from MD simulations (solid line) and their fit-free GCM replicas (dashed line), obtained within the five-variable dynamic model (6): density-density, density-energy, and energy-energy for liquid iron at the wave numbers $k = 0.267$ Å^{-1} (left) and $k = 2.920$ Å^{-1} (right). The time scale for reduced unit is 0.78115 ps.

$F_{ee}(k,t)$ with their theoretical GCM replicas (8) for two wave numbers. One can see that the strongly oscillating form of the density-density and density-energy time correlation functions close to the hydrodynamic regime are well reproduced as well as solely as a relaxation form of the time correlation functions in the region of so-called deGennes slowing-down of density fluctuations close to the first sharp diffraction peak of $S(k)$. This perfect reproduction of the MD time correlation functions by their theoretical GCM replicas is provided by the high number of the sum rules satisfied by expression (9). The density-density time correlation functions within the dynamic model (6) exactly match the first five frequency moments (short-time behavior) and zero time moment of corresponding MD functions. For energy-energy time correlation functions, only the first three frequency moments and zero time moment exactly match the MD functions, because only the first time derivative of hydrodynamic variable of energy (or heat) density is present is the set (6).

The perfect reproduction of the MD time correlation functions by their theoretical GCM replicas in a wide region of wave numbers (see Fig. 2) means that the five-variable model is correct for description of the relaxation processes and collective excitations in liquid Fe at 1843 K.

C. Longitudinal and transverse collective excitations

Longitudinal dynamics of pure liquids on macroscopic spatial and time scales is completely described by hydrodynamic theory in terms of contributions from a single heat relaxation mode and acoustic collective excitations. Therefore any successful generalized hydrodynamic theory must lead to correct hydrodynamic asymptotes of collective modes in the long-wavelength limit.

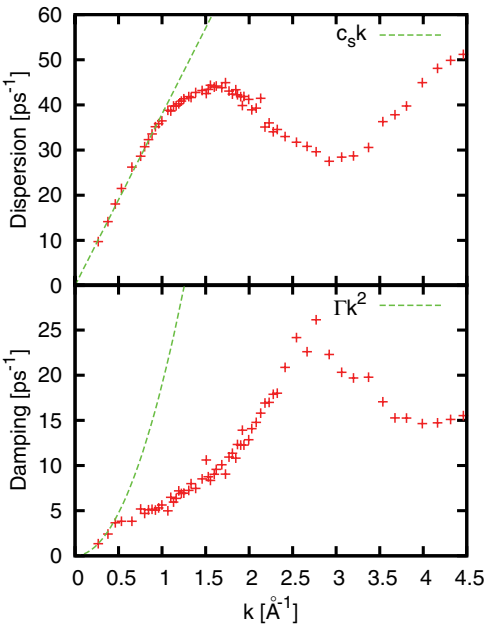

FIG. 3. (Color online) Dispersion and damping of collective excitations in liquid iron at 1843 K, obtained from simulations with EAM potential and GCM analysis. The straight line in the top panel corresponds to hydrodynamic dispersion law with experimental value of speed of sound 3800 m/s. In the bottom panel, the quadratic dependence on k of damping permits to estimate the damping coefficient $\Gamma = 19.1$ Å^2/ps.

In Fig. 3, the calculated dispersion $\omega_s(k)$ and damping $\sigma_s(k)$ of acoustic excitations are shown. In the long-wavelength limit, the dispersion and damping tend to hydrodynamic asymptotes (shown by dashed lines in Fig. 3):

$$\omega_s^{\mathrm{hyd}}(k) = c_s k, \qquad \sigma_s^{\mathrm{hyd}}(k) = \Gamma k^2,$$

where c_s is the adiabatic speed of sound and Γ is the sound damping coefficient

$$\Gamma = \tfrac{1}{2}[D_L + (\gamma - 1)D_T],$$

where D_L and D_T are the kinematic viscosity and thermal diffusivity. One can see that the obtained dispersion in long-wavelength region is very close to the linear dependence with the experimental value of the speed of sound of 3800 m/s.[7] The estimated from the hydrodynamic asymptote damping coefficient Γ is 1.91×10^{-7}m^2/s. We would like to stress that the experimental measurements of speed of sound in liquid systems are very sensitive to the temperature and pressure and one can expect the error bars up to 10% for the reported in the literature values. Indeed, in Ref. 44, there are values of 4400 and 3985 m/s for c_s of liquid Fe at melting point. Perhaps future classical and *ab initio* MD simulations of liquid Fe close to melting point will provide more information on the adiabatic speed of sound in the particular ranges of pressures and temperatures.

Beyond the hydrodynamic regime the dispersion $\omega_s(k)$ of collective excitations deviates from the linear dispersion law. One can see around $k \sim 0.6$ Å^{-1} a shift towards higher energies with respect to the dashed line in the top panel of in Fig. 3. This deviation is called the "positive dispersion" and as it was shown in Ref. 40, the nonhydrodynamic structural

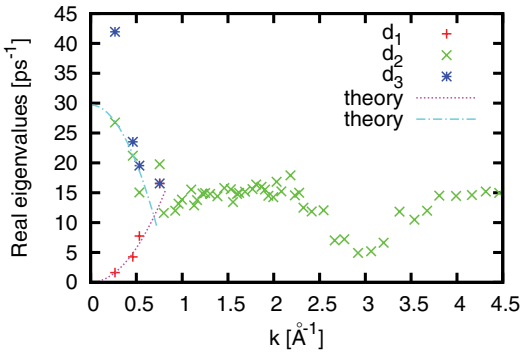

FIG. 4. (Color online) Real eigenvalues that correspond to leading relaxation processes in longitudinal dynamics. The lines in small-k region correspond to analytical long-wavelength asymptotes of relaxation processes.[40,41]

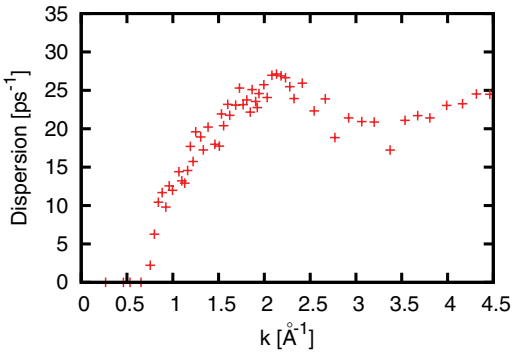

FIG. 5. (Color online) Dispersion of nonhydrodynamic collective propagating modes that correspond to heat waves in liquid iron at 1843 K.

relaxation is responsible for this change from hydrodynamic to high-frequency behavior in sound dispersion. The sound damping in this region also shows a strong deviation from the hydrodynamic asymptote. For the short-wavelength collective excitations, the standard minimum of $\omega_s(k)$ is observed in the region of deGennes slowing-down of density fluctuations. This minimum in the dispersion occurs together with the strong increase of sound damping, that corresponds to the strong scattering of collective excitations on the cages of nearest atoms.

Among the five eigenvalues of the generalized hydrodynamic matrix we obtained for $k < 0.72$ Å^{-1} three real eigenvalues in addition to a pair of complex-conjugated sound modes. For larger wave numbers, the eigenvalues had only one real value and two pairs of complex-conjugated numbers, corresponding to acoustic modes and nonhydrodynamic heat waves. First, we will analyze real eigenvalues. In Fig. 4, we show the obtained real eigenvalues that correspond to relaxation processes in liquid Fe. We would like to remind that the real eigenvalue has the meaning of the inverse relaxation time of corresponding process on the spatial scale $L \sim 2\pi/k$. The lowest real eigenmode is easy to identify. It has the hydrodynamic asymptote $\sim k^2$ and hence this mode corresponds to hydrodynamic thermal relaxation:

$$d_1(k) = D_T k^2, \qquad k \to 0,$$

where D_T is thermal diffusivity. From the hydrodynamic asymptote shown in Fig. 4 by a dotted line, one can estimate the value of thermal diffusivity 2.3×10^{-7} m^2/s. The other relaxing modes can be identified by making use of analytic solutions of the thermoviscoelastic model (6) in the long-wavelength limit.[40] Two relaxing modes $d_2(k)$ and $d_3(k)$ tend to nonzero values in the long-wavelength limit, that means their finite relaxation times on macroscopic distances. Hence in comparison with hydrodynamic modes they do not contribute to dynamics on macroscopic spatial and time scales. This is a general feature of nonhydrodynamic processes. The mode $d_2(k)$ according to analytic solutions corresponds to structural relaxation and behaves in long-wavelength limit as[47]

$$d_2(k) = \frac{c_\infty^2 - c_s^2}{D_L} - D_L k^2 + (\gamma - 1)\Delta k^2, \qquad (10)$$

where c_∞ is the high-frequency speed of sound, and Δ is a factor due to coupling between the modes $d_2(k)$ and $d_3(k)$. One can see in Fig. 4, that the MD results nicely reproduce the analytical long-wavelength behavior of $d_2(k)$ tending to the value of inversed relaxation time of structural relaxation 29.7 ps^{-1}, which means much smaller relaxation time in comparison with hydrodynamic relaxation processes. The relaxing more $d_3(k)$ is of thermal origin and corresponds to relaxation of heat current. The $d_3(k)$ usually tends to higher values then $d_2(k)$, however it decays with wave number faster. Namely, the decay rate of the nonhydrodynamic mode $d_3(k)$ defines the region of wave numbers where exist two relaxation processes of heat origin. In Fig. 4, one can see that for wave numbers $k > 0.72$ Å^{-1}, the main contribution to the relaxation of the density-density correlations comes from the only relaxing mode $d_2(k)$. This is in contrast with hydrodynamic region where the main contribution to the central peak of dynamic structure factor is of thermal origin (lowest relaxing mode). For large wave numbers, mainly the structural relaxation, as the most slow relaxation process, defines the central peak of dynamic structure factor.

For wave numbers $k > 0.72$ Å^{-1}, liquid Fe can support heat waves that provide another mechanism of heat transfer on nanoscale. In Fig. 5, we show the imaginary part (dispersion) of complex-conjugated pair of eigenvalues obtained in addition to the acoustic modes. The absence of heat waves in the long-wavelength region is in complete agreement with hydrodynamics—similarly as this is for the case of transverse sound—liquids do not support the long-wavelength heat waves.[48] The issue of existence on nanoscale heat waves in liquids and their detection is timely because for solids these collective modes were experimentally indentified.[49,50] The propagation gap dispersion of heat waves in liquid Fe shown in Fig. 5 gives evidence that these collective modes can take part in heat transfer on the distances not larger ~9 Å. On larger distances, the heat relaxation processes $d_1(k)$ and $d_3(k)$ play the main role in heat transfer. The microscopic theory of heat waves in liquid metals[39,51] can explain the existing propagating gap for the heat waves and reveals factors that define its width in wave number region. The issue of contributions from heat waves to dynamic structure factors will be discussed in the next section.

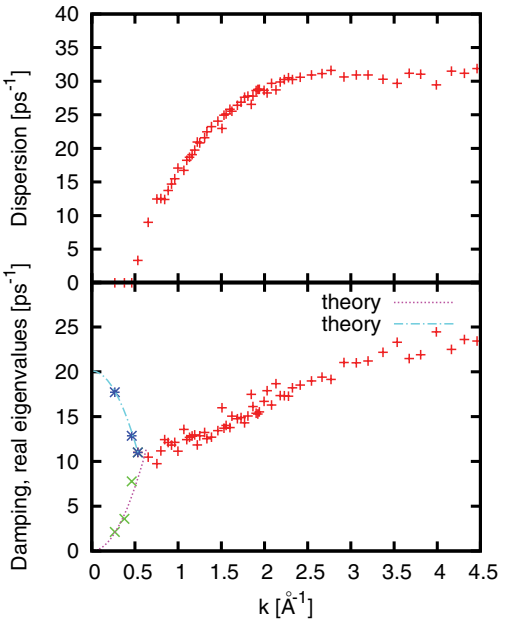

FIG. 6. (Color online) Dispersion and damping of collective shear waves (plus symbols) and main relaxation processes of transverse dynamics in liquid iron at 1843 K. The lines in small-k region correspond to analytical long-wavelength asymptotes of relaxation processes.[42]

Another type of nonhydrodynamic collective excitations that exist on nanoscales are the shear waves in liquids. The spectrum of collective modes for transverse dynamics was obtained by the GCM approach using the extended set of transverse dynamic variables (7). The dispersion of shear waves in liquid Fe is shown in the top panel of Fig. 6, while damping of shear waves and transverse relaxing modes are shown in the bottom panel. In agreement with hydrodynamics, the liquids do not support macroscopic transverse sound, therefore for $k < 0.5$ Å^{-1} there exists a propagation gap for shear waves in liquid Fe. One should note that the widths of propagation gaps for shear and heat waves do not correlate since they are defined by collective processes of different origin. In the long-wavelength region, there exist two transverse relaxing modes and their wave number dependence nicely corresponds to expected behavior from analytical results.[42] The dispersion of shear waves is quite different from the dispersion of longitudinal acoustic excitations. Except the existing propagation gap the transverse collective excitations have very flat dispersion in the short-wavelength region in contrast to strongly nonmonotonic behavior of dispersion of longitudinal modes (see Fig. 3). This is again in agreement with the expected asymptotes for short-wavelength transverse current fluctuations predicted in Ref. 42.

D. Mode contributions to the dynamic structure factors

The GCM approach makes possible to study contributions from different collective modes—relaxing and collective excitations—to dynamic structure factors. The GCM expression for the density-density time correlation function is connected with the dynamic structure factor via time Fourier transformation. This yields the expression for $S(k,\omega)$, that is a direct extension of the dynamic structure factor in hydrodynamic limit:[28,29]

$$\frac{S(k,\omega)}{S(k)} = \sum_{\alpha=1}^{3(1)} A_{nn}^{\alpha}(k)\frac{2d_{\alpha}(k)}{\omega^2 + d_{\alpha}^2(k)} + \sum_{\pm,\alpha=1}^{1(2)} \left\{ B_{nn}^{\alpha}(k)\frac{\sigma_{\alpha}(k)}{[\omega \pm \omega_{\alpha}(k)]^2 + \sigma_{\alpha}^2(k)} \pm D_{nn}^{\alpha}(k)\frac{\omega \pm \omega_{\alpha}(k)}{[\omega \pm \omega_{\alpha}(k)]^2 + \sigma_{\alpha}^2(k)} \right\}. \quad (11)$$

Here, the amplitudes of mode contributions (or as called in Ref. 52 mode strengths) are dependent on wave number: $A_{nn}^{\alpha}(k)$ describes contribution from the α-s relaxing mode to the central peak of $S(k,\omega)$, $B_{nn}^{\alpha}(k)$ is a symmetric contribution from the corresponding propagating mode to the side peaks of $S(k,\omega)$, and $D_{nn}^{\alpha}(k)$ are so-called non-Lorentzian corrections[45] responsible for the asymmetry of Brillouin peaks. Note that the non-Lorentzian corrections are vanishing in the long-wavelength limit, while the mode strengths $A_{nn}^{\alpha}(k)$ and $B_{nn}^{\alpha}(k)$ of hydrodynamic modes tend in $k \to 0$ limit to their values predicted by hydrodynamics.

For the case of liquid Fe, the strengths of leading processes contributing to the shape of $S(k,\omega)$ are shown in Fig. 7. As it follows from the wave number dependence of the mode strengths the hydrodynamic collective processes: acoustic excitations and heat relaxation $d_1(k)$—tend to the hydrodynamic values $1/\gamma$ and $1 - 1/\gamma$, respectively (see Fig. 7). The obtained in this study wave number dependence of generalized ratio $\gamma(k)$ tends in the long-wavelength limit to a value ~1.40 and is in good agreement of experimental estimate from analysis of Landau-Placzek ratio of IXS-measured dynamic structure factors.[7] The values of mode strengths from acoustic excitations and heat relaxation $d_1(k)$ tend to the values $B_{nn}^{\text{sound}}(k \to 0) \sim 0.72$ and $A_{nn}^{1}(k \to 0) \sim 0.28$ as it is seen from Fig. 7.

The mode strengths from the non-hydrodynamic processes tend to zero in the long-wavelength limit that means the

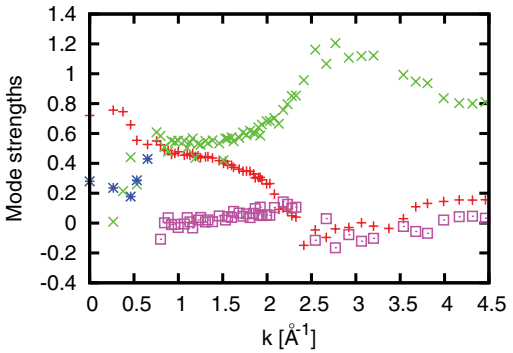

FIG. 7. (Color online) Mode strengths of hydrodynamic and nonhydrodynamic collective modes in dynamic structure factors of liquid iron at 1843 K: plus symbols are sound excitations, open boxes are nonhydrodynamic heat waves, stars are hydrodynamic heat relaxation $d_1(k)$, and cross symbols are structural relaxation $d_2(k)$. Hydrodynamic results for contributions from acoustic modes and heat relaxation are shown at $k = 0$ by symbols plus and star, respectively.

complete agreement with hydrodynamics. However, the nonhydrodynamic modes become very important beyond the hydrodynamic region. At $k \sim 0.5$ Å^{-1}, there exists a crossover in mode strengths $A^{\alpha}_{nn}(k)$ to the central peak of dynamic structure factors: the contribution from structural relaxation becomes the leading one and completely defined the central peak of $S(k,\omega)$ for large wave numbers. The contribution from acoustic collective excitations drops from its hydrodynamic value $1/\gamma$ to very low level and practically it is not important in the region of deGennes slowing down of density fluctuations. In this region, only the one-peak shape of $S(k,\omega)$ is observed that is defined almost completely by structural relaxation. The nonhydrodynamic heat waves marginally contribute to the dynamic structure factors and therefore cannot be detected by scattering experiments. However, very recently it was shown[53] that analysis of "positive dispersion" obtained from the peak position of $S(k,\omega)$ or current spectral function $C^{L}(k,\omega)$ can keep information from coupling between heat waves and high-frequency sound, though this was found for not very dense liquids. For the case of liquid Fe, the heat waves practically do not contribute to the shape of $S(k,\omega)$.

IV. CONCLUSIONS

We reported the fit-free analysis of collective dynamics from MD simulations of liquid iron at temperature 1843 K performed with embedded-atom potentials. The shape of density-density, density-energy, and energy-energy time correlation functions was analyzed by a five-variable dynamic model of generalized hydrodynamics. The obtained results give evidence that the embedded-atom model for liquid Fe proposed in Ref. 12 nicely describes the collective dynamics of iron even not far above the ambient melting point.

The main results of this study are the following. (i) We found that the applied embedded-atom potential for iron reasonably reproduces heat fluctuations resulting in the value of the ratio of specific heats γ close to 1.4, which is in very good agreement with the value obtained by Hosokawa *et al*. from IXS experiments.[7] (ii) The obtained dispersion of collective excitations tends in the long-wavelength limit to the hydrodynamic dispersion law with an estimated speed of sound very close to the experimental value of 3800 m/s.[7] (iii) We obtained among the dynamic eigenmodes the nonhydrodynamic collective excitations: shear and heat waves, which do not exist on macroscopic distances, however, they can propagate in liquid iron with wave numbers larger than ∼0.5 and 0.72 Å^{-1}, respectively. (iv) The detailed analysis of contributions to the dynamic structure factors, obtained from the eigenvectors associated with corresponding eigenvalues, was performed and revealed the good agreement with hydrodynamic asymptotes for acoustic modes and heat relaxation. The heat waves practically do not contribute to the $S(k,\omega)$.

ACKNOWLEDGMENTS

T.B. was partially supported by the NASU Program "Fundamental properties of matter in a wide range of spatial and time scales." A.B. acknowledges the financial support from the Swedish Research Council (VR).

[1] W. W. Anderson and T. J. Ahrens, J. Geophys. Res. **99**, 4273 (1994).
[2] P. M. Nasch, M. H. Manghnani, and R. A. Secco, J. Geophys. Res. **99**, 4285 (1994).
[3] P. M. Nasch and S. G. Steinemann, Phys. Chem. Liq. **29**, 43 (1995).
[4] M. D. Rutter, R. A. Secco, H. Liu, T. Uchida, M. L. Rivers, S. R. Sutton, and Y. Wang, Phys. Rev. B **66**, 060102(R) (2002).
[5] R. A. Secco, M. D. Rutter, S. P. Balog, H. Liu, D. C. Rubie, T. Uchida, D. Frost, Y. Wang, M. Rivers, and S. R. Sutton, J. Phys.: Condens. Matter **14**, 11325 (2002).
[6] G. Shen, V. B. Prakapenka, M. L. Rivers, and S. R. Sutton, Phys. Rev. Lett. **92**, 185701 (2004).
[7] S. Hosokawa, M. Inui, K. Matsuda, D. Ishikawa, and A. Q. R. Baron, Phys. Rev. B **77**, 174203 (2008).
[8] S. Hosokawa, M. Inui, K. Matsuda, D. Ishikawa, and A. Q. R. Baron, J. Phys.: Conf. Series. **98**, 022004 (2008).
[9] G. A. de Wijs, G. Kresse, L. Vocadlo, D. Dobson, D. Alfe, M. J. Gillan, and G. D. Price, Nature (London) **392**, 805 (1998).
[10] D. Alfe, M. J. Gillan, and G. D. Price, Nature (London) **401**, 462 (1999).
[11] D. Alfe, G. Kresse, and M. J. Gillan, Phys. Rev. B **61**, 132 (2000).
[12] A. B. Belonoshko, R. Ahuja, and B. Johansson, Phys. Rev. Lett. **84**, 3638 (2000).
[13] H. K. Mao, J. Xu, V. V. Struzhkin, J. Shu, R. J. Hemley, W. Sturhahn, M. Y. Hu, E. E. Alp, L. Vocadlo, D. Alfe, G. D. Price, M. J. Gillan, M. Schwoerer-Böhning, D. Häusermann, P. Eng, G. Shen, H. Giefers, R. Lübbers, and G. Wortmann, Science **292**, 914 (2001).
[14] L. Koci, A. B. Belonoshko, and R. Ahuja, Phys. Rev. B **73**, 224113 (2006).
[15] C. Desgranges and J. Delhommelle, Phys. Rev. B **76**, 172102 (2007).
[16] W. Luo, B. Johansson, O. Eriksson, S. Arapan, P. Souvatzis, M. I. Katznelson, and R. Ahuja, Proc. Natl. Acad. Sci. USA **107**, 9962 (2010).
[17] A. B. Belonoshko, T. Bryk, and A. Rosengren, Phys. Rev. Lett. **104**, 245703 (2010).
[18] A. B. Belonoshko, S. Arapan, and A. Rosengren, J. Phys.: Condens. Matter **23**, 485402 (2011).
[19] A. B. Belonoshko, N. V. Skorodumova, S. Davis, A. N. Osiptsov, A. Rosengren, and B. Johansson, Science **316**, 1603 (2007).
[20] A. B. Belonoshko, N. V. Skorodumova, A. Rosengren, and B. Johansson, Science **319**, 797 (2008).
[21] A. B. Belonoshko, Condens. Matter Phys. **13**, 23605 (2010).
[22] M. Pozzo, C. Davies, D. Gubbins, and D. Alfe, Nature (London) **485**, 355 (2012).
[23] D. Alfe, G. D. Price, and M. J. Gillan, Phys. Rev. B **65**, 165118 (2002).
[24] P. Söderlind, J. A. Moriarty, and J. M. Wills, Phys. Rev. B **53**, 14063 (1996).
[25] M. M. G. Alemany, C. Rey, and L. J. Gallego, Phys. Rev. B **58**, 685 (1998).

[26]M. D. Ruiz-Martin, M. Jimenez-Ruiz, M. Plazanet, F. J. Bermejo, R. Fernandez-Perea, and C. Cabrillo, Phys. Rev. B **75**, 224202 (2007).
[27]S. Cazzato, T. Scopigno, S. Hosokawa, M. Inui, W.-C. Pilgrim, and G. Ruocco, J. Chem. Phys. **128**, 234502 (2008).
[28]J.-P. Boon and S. Yip, *Molecular Hydrodynamics* (McGraw-Hill, New-York, 1980).
[29]J.-P. Hansen and I. R. McDonald, *Theory of Simple Liquids* (Academic, London, 1986).
[30]T. Scopigno, G. Ruocco, and F. Sette, Rev. Mod. Phys. **77**, 881 (2005).
[31]T. Scopigno, U. Balucani, G. Ruocco, and F. Sette, J. Phys.: Condens. Matter **12**, 8009 (2000).
[32]T. Scopigno, G. Ruocco, F. Sette, and G. Viliani, Phys. Rev. E **66**, 031205 (2002).
[33]T. Scopigno, A. Filipponi, M. Krisch, G. Monaco, G. Ruocco, and F. Sette, Phys. Rev. Lett. **89**, 255506 (2002).
[34]D. J. Gonzalez, L. E. Gonzalez, J. M. Lopez, and M. J. Stott, Phys. Rev. E **69**, 031205 (2004).
[35]D. J. Gonzalez, L. E. Gonzalez, J. M. Lopez, and M. J. Stott, J. Phys.: Condens. Matter **17**, 1429 (2005).
[36]W. Schirmacher and H. Sinn, Condens. Matter Phys. **11**, 127 (2008).
[37]B. Schmid and W. Schirmacher, J. Phys.: Condens. Matter **23**, 254211 (2011).
[38]I. M. Mryglod, I. P. Omelyan, and M. V. Tokarchuk, Mol. Phys. **84**, 235 (1995).
[39]T. Bryk, Eur. Phys. J. Spec. Top. **196**, 65 (2011).
[40]T. Bryk, I. Mryglod, T. Scopigno, G. Ruocco, F. Gorelli, and M. Santoro, J. Chem. Phys. **133**, 024502 (2010).
[41]T. Bryk and I. Mryglod, Condens. Matter Phys. **7**, 471 (2004).
[42]T. Bryk and I. Mryglod, Phys. Rev. E **62**, 2188 (2000).
[43]I. M. de Schepper, E. G. D. Cohen, C. Bruin, J. C. van Rijs, W. Montfrooij, and L. A. de Graaf, Phys. Rev. A **38**, 271 (1988).
[44]T. Iida and R. I. L. Guthrie, *The Physical Properties of Liquid Metals*, (Clarendon, Oxford, 1988).
[45]C. Cohen, J. W. H. Sutherland, and J. M. Deutch, Phys. Chem. Liq. **2**, 213 (1971).
[46]T. Bryk and I. Mryglod, Phys. Rev. E **64**, 032202 (2001).
[47]T. Bryk and I. Mryglod, Condens. Matter Phys. **11**, 139 (2008).
[48]D. D. Joseph and L. Preziosi, Rev. Mod. Phys. **61**, 41 (1989).
[49]V. Narayanamurti and R. C. Dynes, Phys. Rev. Lett. **28**, 1461 (1972).
[50]A. Koreeda, R. Takanao, and S. Saikan, Phys. Rev. Lett. **99**, 265502 (2007).
[51]T. Bryk and I. Mryglod, Phys. Rev. E **63**, 051202 (2001).
[52]N. H. March and M. P. Tosi, *Coulomb Liquids* (Academic Press, London, NewYork, 1984).
[53]F. Gorelli *et al*. (unpublished).